

The B-site ordering in RFe$_{0.5}$Cr$_{0.5}$O$_3$ ceramics and its effect on magnetic properties

Li Hou(侯利), Lei Shi(石磊), Liping Yang(杨利平), Yiqiang Liu(刘义强), Zhitao Li(李志涛), and Lanxiang Meng(孟蓝翔)

Citation: Chin. Phys. B, 2024, 33 (**10**): 108101. DOI: 10.1088/1674-1056/ad641e
Journal homepage: http://cpb.iphy.ac.cn; http://iopscience.iop.org/cpb

What follows is a list of articles you may be interested in

High-pressure and high-temperature sintering of pure cubic silicon carbide: A study on stress-strain and densification

Jin-Xin Liu(刘金鑫), Fang Peng(彭放), Guo-Long Ma(马国龙), Wen-Jia Liang(梁文嘉), Rui-Qi He(何瑞琦), Shi-Xue Guan(管诗雪), Yue Tang(唐越), and Xiao-Jun Xiang(向晓君)
Chin. Phys. B, 2023, 32 (**9**): 098101. DOI: 10.1088/1674-1056/aca6d4

Progress in functional studies of transition metal borides

Teng Ma(马腾), Pinwen Zhu(朱品文), and Xiaohui Yu(于晓辉)
Chin. Phys. B, 2021, 30 (**10**): 108103. DOI: 10.1088/1674-1056/ac1925

Properties of B_4C-TiB_2 ceramics prepared by spark plasma sintering

Jingzhe Fan(范静哲), Weixia Shen(沈维霞), Zhuangfei Zhang(张壮飞, Chao Fang(房超), Yuewen Zhang(张跃文), Liangchao Chen(陈良超), Qianqian Wang(王倩倩), Biao Wan(万彪), and Xiaopeng Jia(贾晓鹏)
Chin. Phys. B, 2021, 30 (**3**): 038105. DOI: 10.1088/1674-1056/abd7d8

Vertical GaN Shottky barrier diode with thermally stable TiN anode

Da-Ping Liu(刘大平), Xiao-Bo Li(李小波), Tao-Fei Pu(蒲涛飞), Liu-An Li(李柳暗), Shao-Heng Cheng(成绍恒), and Qi-Liang Wang(王启亮)
Chin. Phys. B, 2021, 30 (**3**): 038101. DOI: 10.1088/1674-1056/abc547

Structural stability and vibrational characteristics of CaB_6 under high pressure

Mingkun Liu(刘明坤), Can Tian(田灿), Xiaoli Huang(黄晓丽), Fangfei Li(李芳菲), Yanping Huang(黄艳萍), Bingbing Liu(刘冰冰), Tian Cui(崔田)
Chin. Phys. B, 2019, 28 (**6**): 068101. DOI: 10.1088/1674-1056/28/6/068101

The B-site ordering in RFe$_{0.5}$Cr$_{0.5}$O$_3$ ceramics and its effect on magnetic properties

Li Hou(侯利)[1,†], Lei Shi(石磊)[2,‡], Liping Yang(杨利平)[2], Yiqiang Liu(刘义强)[1], Zhitao Li(李志涛)[1], and Lanxiang Meng(孟蓝翔)[1]

[1] *School of Materials Science and Engineering, Anyang Institute of Technology, Anyang* 455000, *China*
[2] *Hefei National Laboratory for Physical Sciences at Microscale, University of Science and Technology of China, Hefei* 230026, *China*

(Received 9 April 2024; revised manuscript received 17 June 2024; accepted manuscript online 17 July 2024)

To insight into the B-site ordering in RFe$_{0.5}$Cr$_{0.5}$O$_3$ ceramics, a series of RFe$_{0.5}$Cr$_{0.5}$O$_3$ ceramics (R = La, Y, Lu) were synthesized by the sol–gel method, and the structural and magnetic properties were systemically investigated. By using the Rietveld refinement of all samples, it is found that the structural distortion is increased as the R ionic radius decreases, leading to the weakened interactions between Fe/Cr ions. Moreover, the Fe and Cr are arranged in disorder in LaFe$_{0.5}$Cr$_{0.5}$O$_3$, but partially ordered in YFe$_{0.5}$Cr$_{0.5}$O$_3$ and LuFe$_{0.5}$Cr$_{0.5}$O$_3$, showing an increasing trend of the proportion of ordered domains with the decrease of R ionic radius. Through fitting the temperature-dependent magnetizations, it is identified that the magnetization reversal (MR) in disorder LaFe$_{0.5}$Cr$_{0.5}$O$_3$ is resulted from the competition between the moments of Cr and Fe sublattices. In the partially ordered YFe$_{0.5}$Cr$_{0.5}$O$_3$ and LuFe$_{0.5}$Cr$_{0.5}$O$_3$ ceramics, because of the presence of Fe–O–Cr networks in the ordered domains whose moment is antiparallel to that of Fe–O–Fe and Cr–O–Cr in the disordered domains, the compensation temperature $T_{\rm comp}$ of MR is increased by nearly 50 K. These results suggest that the changing of R-site ions could be used very effectively to modify the Fe–O–Cr ordering, apart from the structural distortion, which has a direct effect on the magnetic exchange interactions in RFe$_{0.5}$Cr$_{0.5}$O$_3$ ceramics. Then at values of composition where ordered domains are expected to be larger in number as compared to disordered domains and with a weaker structural distortion, one can expect a higher transition temperature $T_{\rm comp}$, providing a different view for adjustment of the magnetic properties of RFe$_{0.5}$Cr$_{0.5}$O$_3$ ceramics for practical applications.

Keywords: RFe$_{0.5}$Cr$_{0.5}$O$_3$ ceramics, structural distortion, B-site ordering, magnetization reversal

PACS: 81.05.Je, 61.66.–f, 64.60.Cn, 75.60.Jk **DOI:** 10.1088/1674-1056/ad641e

1. Introduction

Perovskites-type oxides ABO_3, displaying a wide range of properties (superconductivity, colossal magnetoresistance, multiferroic behavior, etc.), arguably represent the most important family of complex oxides.[1] Among them, rare-earth orthoferrites (RFeO$_3$) and orthochromites (RCrO$_3$) (R = rare-earth element) have always been paid much attention due to the unique magnetic properties.[2–5] Magnetization reversal (MR, also known as negative magnetization) is a fascinatingly interesting magnetic behavior in RFeO$_3$ and RCrO$_3$, which is a phenomenon where the net magnetization changes its sign and is zero at the compensation temperature ($T_{\rm comp}$).[6] It provides the possibility of preparing the thermally-assisted magnetic random access memory and spin resolution devices.[7–9] However, the temperature $T_{\rm comp}$ is very low,[10–12] which does not meet the practical application requirements. Surprisingly, many remarkable properties were observed in RFe$_{0.5}$Cr$_{0.5}$O$_3$ ceramics, such as magnetocaloric effect,[13,14] negative thermal expansion,[15] and magnetoelectric effect.[16,17] The reversed exchange-bias (EB) effect was observed in LuFe$_{0.5}$Cr$_{0.5}$O$_3$ which had never been seen in LuFeO$_3$ and LuCrO$_3$.[18] These findings sparked a particular interest in RFe$_{0.5}$Cr$_{0.5}$O$_3$ ceramics as a potential material to meet the increasing demand for multifunctional devices.

Crystal structure and defects are one of the most attractive characteristics in perovskite materials.[19] Generally, half substituting of the B-site cations by another cation B′ in ABO_3 materials may take on ordered B–O–B′ arrangements. It is worth noting that B-site ordering has an important impact on the magnetic and electric properties.[1] The dielectric properties of double perovskite Pb$_2$ScTaO$_6$ are sensitive to the changes in the degree of B-site ordering: Relaxor behavior emerges as the B–O–B′ order decreases, while highly ordered samples behave as normal ferroelectrics.[20,21] The spin polarization of half-metallic ferrimagnets Sr$_2$FeMoO$_6$ compounds degrades rapidly as the degree of B-site ordering decreases.[22,23] The combination of ferromagnetism and insulating behavior cannot be realized in mono perovskites, but can be attained in double perovskites.[24,25] Therefore, the B-site ordering may also have the effect on magnetic properties, such as MR, in RFe$_{0.5}$Cr$_{0.5}$O$_3$ ceramics.

However, the B-site ordering in RFe$_{0.5}$Cr$_{0.5}$O$_3$ ceramics has not been systematically studied. In the vast majority of research on RFe$_{0.5}$Cr$_{0.5}$O$_3$ ceramics, the arrangement of Fe and Cr cations is considered to be disordered and the cor-

†Corresponding author. E-mail: 20210023@ayit.edu.cn
‡Corresponding author. E-mail: shil@ustc.edu.cn

© 2024 Chinese Physical Society and IOP Publishing Ltd

responding properties are also explained based on the Fe/Cr disorder.[26–29] Only a few studies suggest that Fe and Cr are arranged in an orderly manner.[16,30] Mo *et al.* have studied the distribution of B-site cations in the perovskite of a d^5–d^3 superexchange system with molecular field theory and Monte Carlo simulation, and revealed that the distribution of Fe/Cr in the majority of systems deviates from the uniform distribution (disordering).[31] Therefore, how the B-site cations are distributed in RFe$_{0.5}$Cr$_{0.5}$O$_3$ ceramics, ordered or disordered, and its effect on magnetic properties is still an open issue.

If R is a magnetic ion, there will be three types of magnetic interactions in RFe$_{0.5}$Cr$_{0.5}$O$_3$ ceramics: R^{3+}–O^{2-}–Fe^{3+}/Cr^{3+}, Fe^{3+}/Cr^{3+}–O^{2-}–Fe^{3+}/Cr^{3+}, R^{3+}–O^{2-}–R^{3+}. Therefore, to study the B-site ordering and the effect on magnetic properties of RFe$_{0.5}$Cr$_{0.5}$O$_3$ ceramics neglecting the influence of R ions, in this paper, a series of RFe$_{0.5}$Cr$_{0.5}$O$_3$ ceramics with R = non-magnetic ions (La, Y, Lu) were synthesized by the sol–gel method, and their structural and magnetic properties were systemically investigated. By refining the crystal structure of all samples, it is found that Fe and Cr were disorderly arranged in RFe$_{0.5}$Cr$_{0.5}$O$_3$ of R = La as same as those in R = Ce, Pr, Nd, Sm,[32] but partially ordered in YFe$_{0.5}$Cr$_{0.5}$O$_3$ and LuFe$_{0.5}$Cr$_{0.5}$O$_3$, showing an increasing trend of proportion of ordered domains as the R ionic radius decreases. Because of the presence of Fe–O–Cr networks in the ordered domains with the moment antiparallel to that of Fe–O–Fe and Cr–O–Cr in the disordered domains, the compensation temperature $T_{\rm comp}$ is increased, which is beneficial for the practical application of materials. These results indicate that the alteration of the R ionic radius can effectively regulate the Fe–O–Cr ordering, which has a significant impact on the magnetic properties of RFe$_{0.5}$Cr$_{0.5}$O$_3$ ceramics.

2. Experimental details

The polycrystalline RFe$_{0.5}$Cr$_{0.5}$O$_3$ (R = La, Y, Lu) ceramics were prepared by the sol–gel method. Typically, stoichiometric amounts of La(NO$_3$)$_3$·nH$_2$O/Y(NO$_3$)$_3$·3H$_2$O/Lu(NO$_3$)$_3$·xH$_2$O, Fe(NO$_3$)$_3$·9H$_2$O and Cr(NO$_3$)$_3$·9H$_2$O were dissolved in ethylene glycol. The citric acid with a molar ratio of 1.5 : 1 to metal nitrates was added into the above mixed solution as a crosslinking agent. The mixed solution was stirred at 100 ℃ for 24 h to form the sol. The sol was then dried at 150 ℃ for 24 h in an oven and decomposed at 400 ℃ for 10 h in air to eliminate the organic matter. Finally, the products were annealed at 1200 ℃ for 2 h to obtain RFe$_{0.5}$Cr$_{0.5}$O$_3$ (R = La, Y, Lu) ceramics.

The x-ray diffraction (XRD, Rigaku SmartLab) with Cu $K\alpha$ (λ = 1.54187 Å) radiation was used to characterize the phase compositions and structures of the samples. The Raman spectra in the backscattering geometry were measured through a JY LABRAMHR Raman spectroscopy with an Ar$^+$ ($\sim$ 532 nm line) laser as an excitation light source. The valence states of the elements were investigated by x-ray photoelectron spectroscopy (XPS, ESCALAB25Xi, Thermo, USA). The magnetic properties were measured on a vibrating sample magnetometer (VSM, Quantum Design, USA) (10 K $\leq T \leq$ 30 K, -5 T $\leq H \leq$ 5 T).

3. Results and discussion

The XRD patterns of the RFe$_{0.5}$Cr$_{0.5}$O$_3$ (R = La, Y, Lu) ceramics are shown in Fig. 1(a). It can be observed that only the perovskite-type phase can be detected with the space group of *Pbnm*. The diffraction peaks are moved toward higher angles ascribed to the monotonic decrease of the unit cell volume with the R^{3+} ionic radius decreasing (La^{3+}: 1.032 Å, Y^{3+}: 0.9 Å, Lu^{3+}: 0.861 Å). In addition, more and more diffraction peaks are clearly observed with the decrease of R^{3+} ionic radius, indicating that the lattice distortion in the materials is intensified. Moreover, the Raman spectra of RFe$_{0.5}$Cr$_{0.5}$O$_3$ (R = La, Y, Lu) ceramics are shown in Fig. 1(b) combined with the Raman spectra of R = Ce, Pr, Nd, Sm detected previously.[32] It can be obviously found that the vibration modes at 200–600 cm^{-1} move to higher wavenumbers with the lanthanide substitution from La to Lu, which is ascribed to the decrease of the unit cell volume and most of the bond lengths closely related to the smaller radius of R^{3+} ions. The vibration mode near 700 cm^{-1} has been attributed to the in-plane symmetric oxygen breathing mode (S) of Fe/CrO$_6$ octahedra,[33,34] which shifts to lower wavenumbers, also indicating that the lattice distortion in RFe$_{0.5}$Cr$_{0.5}$O$_3$ is increased due to the radius of R^{3+} ions decreasing as those shown in other RFe$_{0.5}$Cr$_{0.5}$O$_3$ ceramics.[32,35]

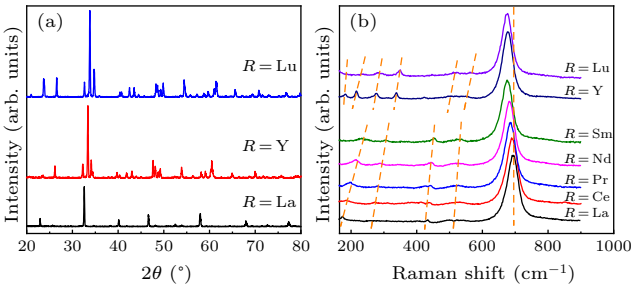


Fig. 1. (a) XRD patterns and (b) Raman spectra of RFe$_{0.5}$Cr$_{0.5}$O$_3$ (R = La, Y, Lu) ceramics.

The temperature-dependent zero-field-cooling (ZFC) and field-cooling (FC) magnetizations $M(T)$ of RFe$_{0.5}$Cr$_{0.5}$O$_3$ (R = La, Y, Lu) ceramics under a field of 100 Oe are shown in Figs. 2(a)–2(c). It can be found that the magnetic characteristics of RFe$_{0.5}$Cr$_{0.5}$O$_3$ (R = La, Y, Lu) compounds are similar, showing a weak ferromagnetic (FM) property due to the canted antiferromagnetic (AFM) arrangement of Fe/Cr spins. Obtained from the corresponding d$M(T)$/dT curves [insets in Figs. 2(a)–2(c)], the AFM Néel temperatures $T_{\rm N}$ for R = La,

Y, and Lu are higher than 300 K, ∼272 K, and 264 K, respectively. This result suggests that the canted AFM ordered temperature decreases with the radius of R^{3+} ions decreasing, which can be attributed to the decreased angle of Fe/Cr–O–Fe/Cr related to the strengthened structural distortion, as shown by XRD and Raman analysis. Below the Néel temperature, MR, the reversal of magnetization under FC mode, is observed in all samples. It is found that the compensation temperatures $T_{\rm comp}$ at which zero magnetization occurs are 183 K, 231 K, and 211 K for R = La, Y, and Lu, respectively, non-monotonically changing with the strengthened structural distortion, which indicates that there are different factors that affect MR in $R{\rm Fe}_{0.5}{\rm Cr}_{0.5}{\rm O}_3$ (R = La, Y, Lu) ceramics. The values of magnetizations under FC mode also take on a non-monotonic change with the decrease of R ion radius, showing an ascending order of La < Lu < Y, which is consistent with the change of compensation temperatures.

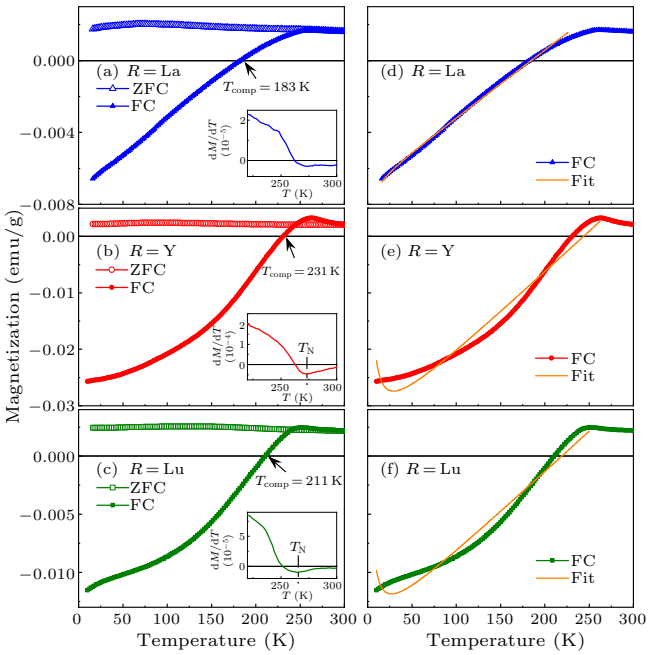


Fig. 2. ZFC, FC magnetizations $M(T)$ and the corresponding d$M(T)$/dT curves (inset) of $R{\rm Fe}_{0.5}{\rm Cr}_{0.5}{\rm O}_3$ ceramics under the magnetic field of 100 Oe: (a) R = La; (b) R = Y; (c) R = Lu; FC $M(T)$ curves along with the fitted data for (d) R = La; (e) R = Y; (f) R = Lu.

The MRs in $R{\rm Fe}_{0.5}{\rm Cr}_{0.5}{\rm O}_3$ ceramics with R = paramagnetic (PM) ions have been systemically investigated before and were ascribed to the antiparallel moments of canted AFM Fe/Cr and PM R sublattices.[32] For the $R{\rm Fe}_{0.5}{\rm Cr}_{0.5}{\rm O}_3$ with R = non-magnetic ions, the magnetic properties are only affected by the canted AFM Fe/Cr–O–Fe/Cr sublattices. Normally, there are two mechanisms arising the canting of AFM moments: the single-ion magnetic anisotropy (SIMA) and the antisymmetric Dzyaloshinskii–Moriya (DM) interaction.[36–38] The canted AFM arrangement with weak FM in $R{\rm FeO}_3$ is due to DM interaction between Fe^{3+} ions,[39] while that in $R{\rm CrO}_3$ is because of the SIMA owing to the effect of t–e hybridization.[40] Therefore, the equal proportion of Fe and Cr with a disordered distribution of Fe^{3+} and Cr^{3+} ions in $R{\rm Fe}_{0.5}{\rm Cr}_{0.5}{\rm O}_3$ brings out the competition between the SIMA and the antisymmetric DM interactions. As reported by Kadomtseva *et al.*,[41] the net moments produced by these two factors are in opposite directions and have different temperature dependence of magnetization. Then, the reversal of magnetization will take place as temperature decreases. In this work, the fitting of $M(T)$ data under FC mode to the competition between the SIMA (Cr moments) and the DM (Fe moments) interactions[36] is shown in Figs. 2(d)–2(f). By taking θ as a spin canting angle due to DM and γ as that due to SIMA, the net magnetic moment of the canted AFM system can be written as

$$M_{\rm net} = 2Ng\mu_{\rm B}|\langle S\rangle|\sin\theta \quad (\sin\theta \approx \theta).$$

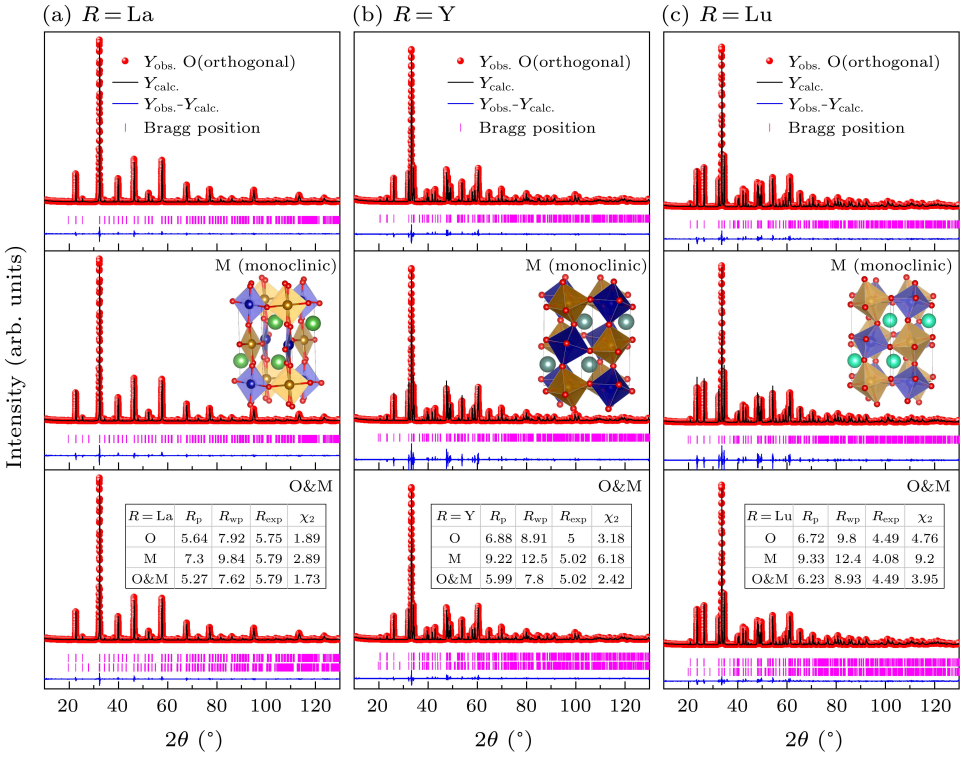
Here, $|\langle S\rangle| = [g\mu_{\rm B}S(S+1)H]/(3k_{\rm B}T)$ for the mean field model. By choosing the reduced constants $\xi = A/J \ll |1$ and $\gamma_{\rm D} = D/(2J)$ (A, J and D are the SIMA constant, AFM coupling constant and DM exchange vector, respectively), the expression for θ becomes

$$\theta \approx \frac{S^2\xi\gamma - \gamma_{\rm D}|\langle S\rangle|^2}{|\langle S\rangle|^2}.$$

It is obvious that the $M(T)$ data of $LaFe_{0.5}Cr_{0.5}O_3$ can be fitted well, but poor fittings are observed for R = Y and Lu samples. Here, it is worth noting that the above fitting theory is based on the disordered arrangement of Fe and Cr ions. However, the Fe and Cr ions with equal proportion in $R{\rm Fe}_{0.5}{\rm Cr}_{0.5}{\rm O}_3$ ceramics may be arranged under the ordered Fe–O–Cr pattern, which will lead to the inapplicability of above fitting theory.

To reflect the arrangement of Fe and Cr ions at B site explicitly, the XRD pattern for all the samples were simulated by the Rietveld method. For many ABO_3 materials with half doped by B′ at B site, when B and B′ are arranged in disorder, the crystal structure belongs to orthogonal space group of *Pbnm*; when B and B′ are orderly arranged, the crystal structure belongs to monoclinic space group of $P2_1/n$.[35] Therefore, the three samples were refined under three circumstances: the orthogonal disordered perovskite with space group of *Pbnm* (O), the monoclinic double/ordered perovskite with space group of $P2_1/n$ (M), the coexistence of ordered and disordered perovskite space groups (O&M), as shown in Fig. 3. The reliability factors of fitting with these three circumstances are summerized in the insets of Fig. 3, from which it can be found that $R{\rm Fe}_{0.5}{\rm Cr}_{0.5}{\rm O}_3$ (R = La, Y, Lu) ceramics can be fitted well with disordered orthogonal phase. The reliability factors of fitting for three samples under completely ordered phase are higher than those under disordered phase. The corresponding crystal structures of completely ordered $R{\rm Fe}_{0.5}{\rm Cr}_{0.5}{\rm O}_3$ (R = La, Y, Lu) ceramics with the $P2_1/n$ phase are illustrated in the insets of Fig. 3 made by VESTA software, showing the tilting of Fe/CrO_6 structure with the

ordered arrangement of Fe and Cr ions in rock salt. However, the Fe/CrO_6 structure in $LaFe_{0.5}Cr_{0.5}O_3$ is found to deviate from the normal octahedron. It is noted that the reliability factor of fitting with O&M is the lowest, indicating that the partially ordered arrangement of Fe and Cr ions is presented in the $RFe_{0.5}Cr_{0.5}O_3$ (R = La, Y, Lu) ceramics. Meanwhile, the structural parameters obtained with the coexistence of ordered and disordered perovskite space group for $RFe_{0.5}Cr_{0.5}O_3$ (R = La, Y, Lu) ceramics are summarized in Table 1. It can be seen that the unit cell volume is decreased monotonically with the radius of R^{3+} ions decreasing. Moreover, the average angle of Fe/Cr–O–Fe/Cr is not 180° due to the tilt of Fe/CrO_6 octahedron and also decreases gradually with the decrease of R^{3+} ionic radius, indicating the enhancement of Fe/CrO_6 octahedron distortion consistent with above analysis. In addition, the proportion of monoclinic phase related to the ordered phase in R = La sample is so small that it can be ignored, while those in R = Y and Lu samples are about 70% and 77%, respectively. These results indicate that Fe and Cr are arranged in disorder in $LaFe_{0.5}Cr_{0.5}O_3$ as the same as those in R = Ce, Pr, Nd, Sm,[32] but partially ordered in $YFe_{0.5}Cr_{0.5}O_3$ and $LuFe_{0.5}Cr_{0.5}O_3$, showing an increasing degree of Fe–O–Cr order with the decrease of R ionic radius. This change in B-site ordering will have an important effect on the magnetic properties of $RFe_{0.5}Cr_{0.5}O_3$ ceramics as discussed in the following.



R = La	R_p	R_{wp}	R_{exp}	χ_2
O	5.64	7.92	5.75	1.89
M	7.3	9.84	5.79	2.89
O&M	5.27	7.62	5.79	1.73

R = Y	R_p	R_{wp}	R_{exp}	χ_2
O	6.88	8.91	5	3.18
M	9.22	12.5	5.02	6.18
O&M	5.99	7.8	5.02	2.42

R = Lu	R_p	R_{wp}	R_{exp}	χ_2
O	6.72	9.8	4.49	4.76
M	9.33	12.4	4.08	9.2
O&M	6.23	8.93	4.49	3.95

Fig. 3. Rietveld refined results of XRD pattern for $RFe_{0.5}Cr_{0.5}O_3$ ceramics: (a) R = La; (b) R = Y; (c) R = Lu.

Ren *et al.*[42] have reported that the Hamiltonian of the magnetic system in an external field can be written in the form

$$\mathcal{H} = \mathcal{H}_a + \mathcal{H}_s + \mathcal{H}_e,$$

where the three terms are for the single spin, the interactions between two spins and the effect by external field, respectively. The main contributor to the interactions between two spins is the nearest-neighbor (NN) interactions that can be divided into the isotropic symmetric, the antisymmetric and anisotropic symmetric exchange interaction, among which the anisotropic symmetric exchange can be omitted since it does not play any important role. Based on this, the energy of the system can be written as

$$\frac{E}{N} = -2AS_z^2 + J\boldsymbol{S}_A \cdot \boldsymbol{S}_B + \boldsymbol{D} \cdot (\boldsymbol{S}_A \times \boldsymbol{S}_B) + \frac{E_f}{N},$$

where the first term is for the SIMA, J and $\boldsymbol{D}$ are the isotropic symmetric exchange integral and the antisymmetric DM exchange vector between NN spins, respectively, as described above, and E_f is a contribution from the weak FM couplings resulted from the external field.

Because of the high concentration of the ordered arrangement of Fe–O–Cr in R = Y and Lu samples, the energy of the system will also be affected by the terms of isotropic symmetric (J) and the antisymmetric ($\boldsymbol{D}$) exchange interactions in Fe–O–Cr networks: J_{FeCr} and $\boldsymbol{D}_{FeCr}$, in addition to the interactions in the Fe–O–Fe and Cr–O–Cr networks: J_{FeFe}, J_{CrCr} and $\boldsymbol{D}_{FeFe}$, $\boldsymbol{D}_{CrCr}$. The experimental values of the exchange integrals J_{FeFe}, J_{CrCr} and J_{FeCr} have been estimated by Dasari *et al.*[43] All the integrals are positive in sign, referring to AFM interactions (also see Ref. [44]). According

to theoretical predictions and experimental values,[43,45] antisymmetric DM exchange vectors $\boldsymbol{D}_{\mathrm{FeFe}}$ and $\boldsymbol{D}_{\mathrm{CrCr}}$ possess the same sign, but are opposite to the sign of the $\boldsymbol{D}_{\mathrm{FeCr}}$ vector: $\boldsymbol{D}_{\mathrm{FeFe}} \, ||\boldsymbol{D}_{\mathrm{CrCr}}|| - \boldsymbol{D}_{\mathrm{FeCr}}$. Thus, the MR in $R = \mathrm{Y}$ and Lu samples with partial ordered B-site cations may be mainly argued to the competition between the moments of the Fe–Fe and Cr–Cr pairs vs. that of the Fe–Cr pairs, whose magnetic moments exhibit in opposite directions induced by the DM interactions. However, this competition is very weak for $R = \mathrm{La}$ with disordered B-site ions without Fe–Cr pairs, resulting in the raised temperature T_{comp} from 183 K in disorder $R = \mathrm{La}$ to more than 200 K in partial ordered $R = \mathrm{Y}$ and Lu samples. Though the Fe–O–Cr ordered domains present in both $R = \mathrm{Y}$ and Lu samples, but there is a decreased T_{comp} from 231 K in $R = \mathrm{Y}$ to 211 K in $R = \mathrm{Lu}$, which can be ascribed to the weakened interaction of Fe–O–Cr due to the increased distortion with the decreased radius of R ions. In a word, the variation of compensation temperature T_{comp} with the decrease of R ionic radius is the result of the combination and competition of structural distortion and B-site ordering, as shown in Fig. 4. For the values of magnetizations under FC mode of the three samples, it should be decreasing with the increased distortion related to the decrease of R ion radius. Nevertheless, it shows a same trend of values of magnetizations with the compensation temperature of the three samples, indicating that the partially ordered arrangement of Fe and Cr ions besides the increased distortion has important effects on change of magnetization. Therefore, it is suggested that changing R-site ions could be used effectively to modify the Fe–O–Cr ordering, apart from the structural distortion, which have a direct effect on the parameters of magnetic exchange interactions and corresponding magnetic properties of $R\mathrm{Fe}_{0.5}\mathrm{Cr}_{0.5}\mathrm{O}_3$ ceramics. Then, at values of composition where ordered domains are expected to be large in number as compared to disordered domains and with a weaker structural distortion, one can expect a higher transition temperature T_{comp}.

Table 1. Structural parameters obtained from the Rietveld refinement of the XRD patterns with the coexistence of ordered and disordered perovskite space group (O&M) for $R\mathrm{Fe}_{0.5}\mathrm{Cr}_{0.5}\mathrm{O}_3$ ($R = \mathrm{La}$, Y, Lu) ceramics.

$R\mathrm{Fe}_{0.5}\mathrm{Cr}_{0.5}\mathrm{O}_3$		$R = \mathrm{La}$	$R = \mathrm{Y}$	$R = \mathrm{Lu}$
Orthogonal *Pbnm*	a (Å)	5.53908(7)	5.27187(26)	5.20093(23)
	b (Å)	5.52327(6)	5.55660(23)	5.52095(29)
	c (Å)	7.81344(9)	7.57697(32)	7.52724(51)
	V (Å^3)	239.066(0)	221.958(17)	216.138(23)
	⟨Fe/Cr–O⟩ (Å)	1.9874(2)	2.0048(1)	1.9877(1)
	⟨Fe/Cr–O–Fe/Cr⟩ (°)	159.264(0)	144.247(2)	144.352(2)
Monoclinic $P2_1/n$	*a* (Å)	5.53744(26)	5.26341(4)	5.19578(5)
	b (Å)	5.53285(35)	5.55793(4)	5.52055(5)
	c (Å)	7.85169(56)	7.56950(5)	7.51686(6)
	β (°)	90.0884(54)	90.0122(44)	90.0029(53)
	V (Å^3)	239.065(49)	221.435(3)	215.611(3)
	⟨Fe–O⟩ (Å)	1.9960(1)	2.0004(3)	2.0935(4)
	⟨Cr–O⟩ (Å)	2.3243(1)	1.9976(3)	1.8759(3)
	⟨Fe–O–Cr⟩ (°)	130.005(13)	145.109(2)	144.552(2)
Fract-orthogonal *Pbnm* (%)		98.1(8)	29.7(8)	23.0(11)
Fract-monoclinic $P2_1/n$ (%)		1.9(2)	70.3(9)	77.0(16)
Average ⟨Fe/Cr–O–Fe/Cr⟩ (°)		158.708(7)	144.853(2)	144.506(2)

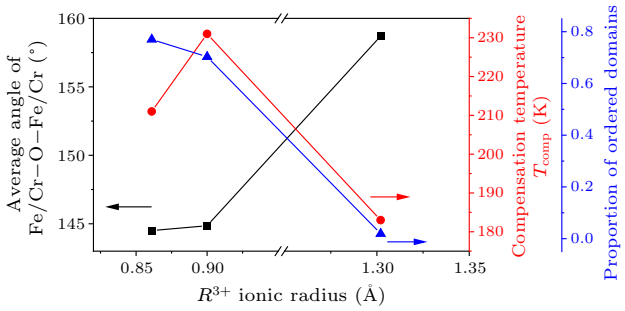


Fig. 4. Average angle of Fe/Cr–O–Fe/Cr, compensation temperature and proportion of ordered domains with the R^{3+} ionic radius for $R\mathrm{Fe}_{0.5}\mathrm{Cr}_{0.5}\mathrm{O}_3$ ($R = \mathrm{La}$, Y, Lu) ceramics.

The magnetic properties affected by the partially ordered structure in $R\mathrm{Fe}_{0.5}\mathrm{Cr}_{0.5}\mathrm{O}_3$ ceramics can be further supported by the isothermal-magnetic hysteresis measurements (see Fig. 5), which were performed at 10 K. As the radius of R ion decreases, the lattice distortion is aggravated, leading to the weakened magnetic interaction and decreased weak FM properties, as observed in Fig. 5, with a decreased remanent magnetization and coercivity field. However, a shift along the field axis in the magnetic hysteresis loops is found in $R = \mathrm{Lu}$ samples, as shown in Fig. 5(c), corresponding to the EB effect, which was also found by Fita *et al.*[18] and explained by the opposite sign of DM exchange vector the Fe–Cr, as compared to that of the Fe–Fe and Cr–Cr, further confirming that there are more Fe and Cr ions in the ordered arrangement in $\mathrm{LuFe}_{0.5}\mathrm{Cr}_{0.5}\mathrm{O}_3$ ceramics.

Generally, the arrangement of two different cations occupying the B site mainly depends on the difference between their valence states or radii.[1,46] Therefore, to confirm the

valence state of Fe and Cr ions, the XPS measurements of $R\mathrm{Fe}_{0.5}\mathrm{Cr}_{0.5}\mathrm{O}_3$ (R = La, Y, Lu) ceramics were carried out. The spectra of the Fe 2p core level for all the samples shown in Fig. 6(a) reveal two Fe 2p core levels. Each of the peaks of Fe 2p core levels can be divided into two distinctive peaks which arise as a result of the presence of Fe^{2+} and Fe^{3+} ions with binding energies of 710.1 eV and 711.5 eV, 723.6 eV and 725.0 eV, respectively.[47] It is obtained that a decrease of Fe^{2+} ions is observed along with the radius of R^{3+} ion decreasing, as listed in Table 2. The core-level XPS Cr 2p spectra [Fig. 6(b)] can also be fitted well with two Cr 2p core levels. The Cr^{6+} species with a single peak at 579.6 eV is overlapped with the multiplet splitting of Cr^{3+} species with binding energies of 575.5 eV, 576.4 eV, 577.06 eV, 578.08 eV, and 579.02 eV.[48,49] It is obtained that with the decrease of the radius of R^{3+} ions, the content of Cr^{6+} ions increase first and then decrease, as shown in Table 2. In addition, the O 1s spectra of all the samples were detected and fitted using three symmetrical peaks at 529.5 eV, 531.2 eV, and 532.4 eV, corresponding to the lattice oxygen (O_L), formed oxygen vacancies (V_O) and absorbed oxygen species on the surface, respectively,[50] as shown in Fig. 6(c). It is found that the content change of Fe^{2+} and Cr^{6+} ions are consistent with that of oxygen vacancies and absorbed oxygen as the radius of R^{3+} ion decreases, respectively, as listed in Table 2. These results indicate that the decrease for Fe^{2+} ions is caused by the reduced oxygen vacancy to maintain the valence states balance, which results from the decreasing radius of R^{3+} ion, similar to the external pressure,[51] while the adsorbed oxygen on the surface is the cause of the presence of Cr^{6+} ions. Then, it can be concluded that the content of Fe^{3+} ions increase with the radius of R^{3+} ions decreasing, and the valence state of Cr ions is mainly trivalent, which is in accordance with other reports,[30] reducing the difference of valence states between Fe and Cr ions. Therefore, the increase of B-site ordering in $R\mathrm{Fe}_{0.5}\mathrm{Cr}_{0.5}\mathrm{O}_3$ ceramics does not result from the difference in valence states or ionic radii between Fe and Cr cations.

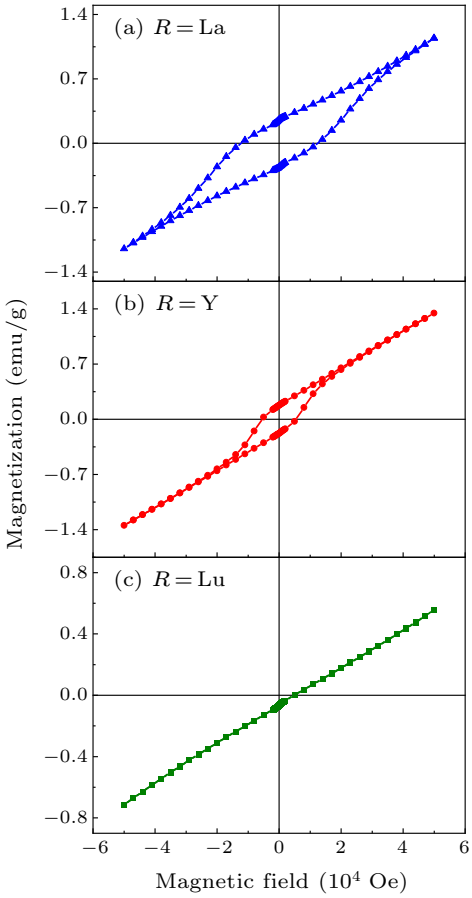


Fig. 5. Magnetic hysteresis loops (M–H) curves of $R\mathrm{Fe}_{0.5}\mathrm{Cr}_{0.5}\mathrm{O}_3$ (R = La, Y, Lu) measured at 10 K.

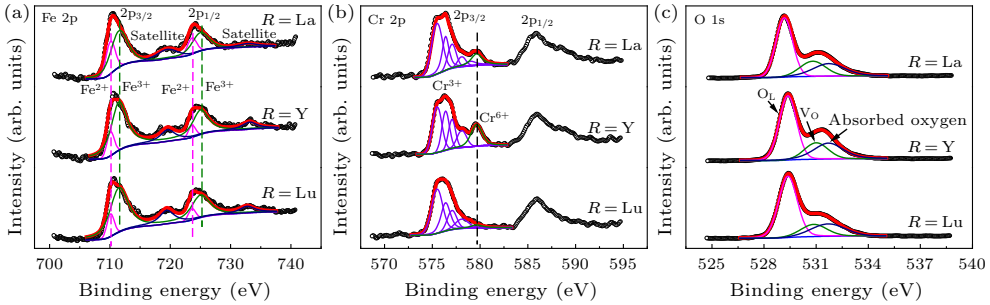


Fig. 6. The XPS spectra of (a) Fe 2p, (b) Cr 2p, and (c) O 1s for $R\mathrm{Fe}_{0.5}\mathrm{Cr}_{0.5}\mathrm{O}_3$ (R = La, Y, Lu) ceramics.

Table 2. Content ratio for Fe, Cr and O ions with different valence states to their total ions in $R\mathrm{Fe}_{0.5}\mathrm{Cr}_{0.5}\mathrm{O}_3$ (R = La, Y, Lu) ceramics.

$R\mathrm{Fe}_{0.5}\mathrm{Cr}_{0.5}\mathrm{O}_3$	Fe^{2+}/Fe_{total}	Cr^{6+}/Cr_{total}	V_O/O_{total}	O_{Abs}/O_{total}
R = La	28.9%	12.6%	27.8%	31.9%
R = Y	24.3%	21.0%	25.2%	35.2%
R = Lu	23.7%	4.1%	21.8%	27.5%

The B-site ordering controlled by A-site cation can also be seen in other systems, while it is attributed to different origins.[52,53] Nevertheless, it seems that these enhanced ordering of B-site cations are all caused by the smaller A-site cations, which is similar to the results in this paper. On the other side, the external pressure during syntheses can also affect the ordering degree of B-site cations.[54] This is due to the fact that the disordered phase increases the volume of the unit cell under the effect of electrostatic repulsion, while the ordered phase helps reduce the volume of the unit cell. Then, under a higher pressure, the ordered phase will become more

favorable. Therefore, in this work, when the radius of A-site ions is smaller, the decrease of the unit cell volume will work similarly to external pressure,[51] which leads to the B-site ions closer and the electrostatic repulsion stronger. Then, the Madelung energy of B-site ordering will increase as the *R*-site ionic radius decreases.[55–57]

4. Conclusion

In summary, to insight into the B-site ordering in $R\mathrm{Fe}_{0.5}\mathrm{Cr}_{0.5}\mathrm{O}_3$ ceramics, a series of $R\mathrm{Fe}_{0.5}\mathrm{Cr}_{0.5}\mathrm{O}_3$ compounds (R = La, Y, Lu) have been synthesized by the sol–gel method, and their structural and magnetic properties are systemically investigated. By refining the crystal structure of all samples, it is found that the structural distortion is increased as *R* ionic radius decreases, leading to the weakened interactions between Fe/Cr ions. In addition, Fe and Cr are arranged in disorder in $\mathrm{LaFe}_{0.5}\mathrm{Cr}_{0.5}\mathrm{O}_3$, but partially ordered in $\mathrm{YFe}_{0.5}\mathrm{Cr}_{0.5}\mathrm{O}_3$ and $\mathrm{LuFe}_{0.5}\mathrm{Cr}_{0.5}\mathrm{O}_3$, showing an increasing trend of proportion of ordered domains with the decrease of *R* ionic radius. Because of the presence of Fe–O–Cr networks in the ordered domains with the moment antiparallel to that of Fe–O–Fe and Cr–O–Cr networks in the disordered domains, the MR in $R\mathrm{Fe}_{0.5}\mathrm{Cr}_{0.5}\mathrm{O}_3$ ceramics are affected directly. The compensation temperatures at which zero magnetization occurs are increased first and then decreased, which is the result of the combination and competition of structural distortion and B-site ordering in $R\mathrm{Fe}_{0.5}\mathrm{Cr}_{0.5}\mathrm{O}_3$ ceramics. These results indicate that the B-site ordering, in addition to the structural distortion, can be effectively regulated by changing the radius of *R*-site ions, which have a direct effect on the magnetic interactions and the corresponding transition temperature of $R\mathrm{Fe}_{0.5}\mathrm{Cr}_{0.5}\mathrm{O}_3$ ceramics. Then, at values of composition where ordered domains are expected to be larger in number as compared to disordered domains and with a weaker structural distortion, one can expect a higher transition temperature T_{comp}, which provides a different view for adjustment of the magnetic properties of $R\mathrm{Fe}_{0.5}\mathrm{Cr}_{0.5}\mathrm{O}_3$ ceramics for practical applications.

Acknowledgments

This project was financially supported by the Natural Science Foundation of Henan Province, China (Grant Nos. 232300420353 and 232300420392), the Key Scientific Research Project of Higher Education of Henan Province (Grant No. 24B140001), the Doctor Scientific Research Initiate Fund of Anyang Institute of Technology (Grant No. BSJ2022010), the National Basic Research Program of China (Grant No. 2009CB939901), and the Henan Provincial Science and Technology Research Project (Grant No. 232102241016).

References

[1] King G and Woodward P M 2010 *J. Mater. Chem.* **20** 5785
[2] Yuan S, Ren W, Hong F, Wang Y, Zhang J, Bellaiche L, Cao S and Cao G 2013 *Phys. Rev. B* **87** 184405
[3] Zhou Z, Guo L, Yang H, Liu Q and Ye F 2014 *J. Alloy. Compd.* **583** 21
[4] Wang S, Wu X, Wang T, Zhang J, Zhang C, Yuan L, Cui X and Lu D 2019 *Inorg. Chem.* **58** 2315
[5] Yin L H, Yang J, Tong P, Luo X, Park C B, Shin K W, Song W H, Dai J M, Kim K H, Zhu X B and Sun Y P 2016 *J. Mater. Chem. C* **4** 11198
[6] Kumar A and Yusuf S M 2015 *Phys. Rep.* **556** 1
[7] Yusuf S M, Kumar A and Yakhmi J V 2009 *Appl. Phys. Lett.* **95** 182506
[8] Mao J, Sui Y, Zhang X, Su Y, Wang X, Liu Z, Wang Y, Zhu R, Wang Y, Liu W and Tang J 2011 *Appl. Phys. Lett.* **98** 192510
[9] Adachi H and Ino H 1999 *Nature* **401** 148
[10] Fita I, Wisniewski A, Puzniak R, Zubov E E, Markovich V and Gorodetsky G 2018 *Phys. Rev. B* **98** 094421
[11] Cao S, Zhao H, Kang B, Zhang J and Ren W 2014 *Sci. Rep.* **4** 5960
[12] Fita I, Wisniewski A, Puzniak R, Markovich V and Gorodetsky G 2016 *Phys. Rev. B* **93** 184432
[13] Yadav K, Kaur G, Sharma M K and Mukherjee K 2020 *Phys. Lett. A* **384** 126638
[14] Yin L H, Yang J, Zhang R R, Dai J M, Song W H and Sun Y P 2014 *Appl. Phys. Lett.* **104** 032904
[15] Pomiro F, Sánchez R D, Cuello G, Maignan A, Martin C and Carbonio R E 2016 *Phys. Rev. B* **94** 134402
[16] Das N, Singh S, Joshi A G, Thirumal M, Reddy V R Gupta L C and Ganguli A K 2017 *Inorg. Chem.* **56** 12712
[17] Rajeswaran B, Mandal P, Saha R, Suard E, Sundaresan A and Rao C N R 2012 *Chem. Mater.* **24** 3591
[18] Fita I, Markovich V, Moskvin A S, Wisniewski A, Puzniak R, Iwanowski P, Martin C, Maignan A, Carbonio R E, Gutowska M U, Szewczyk A and Gorodetsky G 2018 *Phys. Rev. B* **97** 104416
[19] Wu X, Ming C, Shi J, Wang H, West D, Zhang S and Sun Y Y 2022 *Chin. Phys. Lett.* **39** 046101
[20] Baba-Kishi K Z, Woodward P M and Knight K 2001 *Ferroelectrics* **261** 21
[21] Burton B P and Cockayne E 1999 *Phys. Rev. B* **60** R12542
[22] Sarma D D 2001 *Curr. Opin. Solid State Mater. Sci.* **5** 261
[23] Reyes A M, Arredondo Y and Navarro O 2016 *J. Phys. Chem. C* **120** 4048
[24] De Luca G, Spring J, Bashir U, Campanini M, Totani R, Dominguez C, Zakharova A, Döbeli M, Greber T, Rossell M D, Piamonteze C and Gibert M 2021 *APL Mater.* **9** 081111
[25] Rogado N S, Li J, Sleight A W and Subramanian M A 2005 *Adv. Mater.* **17** 2225
[26] Boudad L, Taibi M, Belayachi W, Abd-Lefdil M and Sajieddine M 2022 *Vacuum* **201** 111103
[27] Yin L H, Yang J, Tong P, Luo X, Song W H, Dai J M, Zhu X B and Sun Y P 2017 *Appl. Phys. Lett.* **110** 192904
[28] Mali B, Nair H S, Heitmann T W, Nhalil H, Antonio D, Gofryk K, Bhandari S R, Ghimire M P and Elizabeth S 2020 *Phys. Rev. B* **102** 014418
[29] Yang J, Cao H, Lu Z, Mo J, Zhou Y, Gao K, Xue X, Xia Y and Liu M 2023 *Phys. Status Solidi B* **260** 2300145
[30] Pazhanivelu V, Suriakarthi K, Balogun M S J T, Murugaraj R and Venkateswaran C 2021 *Physica B* **607** 412717
[31] Mo J, Liu M, Xu S, Xia P, Zhang Q, Shen J and Xia Y 2022 *Ceram. Int.* **48** 31309
[32] Hou L, Shi L, Zhao J, Tong R and Xin Y 2021 *J. Phys. Chem. C* **125** 7950
[33] Andreasson J, Holmlund J, Rauer R, Käll M, Börjesson L, Knee C S, Eriksson A K, Eriksson S G, Rübhausen M and Chaudhury R P 2008 *Phys. Rev. B* **78** 235103
[34] Andreasson J, Holmlund J, Knee C S, Käll M, Börjesson L, Naler S, Bäckström J, Rübhausen M, Azad A K and Eriksson S G 2007 *Phys. Rev. B* **75** 104302
[35] Xie C, Shi L, Zhou S, Zhao J, Liu H, Li Y and Yao D 2015 *Surf. Coat. Technol.* **277** 222
[36] Bora T and Ravi S 2013 *J. Appl. Phys.* **114** 033906
[37] Dzyaloshinsky I 1958 *J. Phys. Chem. Solids* **4** 241
[38] Moriya T 1960 *Phys. Rev.* **120** 91
[39] ibschütz M, Shtrikman S and Treves D 1967 *Phys. Rev.* **156** 562
[40] Zhou J S, Alonso J A, Pomjakushin V, Goodenough J B, Ren Y, Yan J Q and Cheng J G 2010 *Phys. Rev. B* **81** 214115

[41] Kadomtseva A M, Moskvin A S, Bostrem I G, Vanklin B M and Hafizova N A 1977 *Sov. Phys. JETP* **72** 2286
[42] Ren Y, Palstra T T M, Khomskii D I, Nugroho A A, Menovsky A A and Sawatzky G A 2000 *Phys. Rev. B* **62** 6577
[43] Dasari N, Mandal P, Sundaresan A and Vidhyadhiraja N S 2012 *Europhys. Lett.* **99** 17008
[44] Billoni O V, Pomiro F, Cannas S A, Martin C, Maignan A and Carbonio R E 2016 *J. Phys.: Condens. Matter* **28** 476003
[45] Moskvin A S 2016 *J. Magn. Magn. Mater.* **400** 117
[46] Ruiz-González M L, Cortés-Gil R, Alonso J M, Hernando A, Vallet-Regí M and González-Calbet J M 2006 *Chem. Mater.* **18** 5756
[47] Hou L, Shi L, Zhao J, Zhou S, Pan S, Yuan X and Xin Y 2019 *J. Alloy. Compd.* **797** 363
[48] Biesinger M C, Payne B P, Grosvenor A P, Lau L W M, Gerson A R and Smart R S C 2011 *Appl. Surf. Sci.* **257** 2717
[49] Lippitz A and Hübert T 2005 *Surf. Coat. Technol.* **200** 250
[50] Ma X, Lu P and Wu P 2018 *J. Alloy. Compd.* **734** 22
[51] Aschauer U, Pfenninger R, Selbach S M, Grande T and Spaldin N A 2013 *Phys. Rev. B* **88** 054111
[52] Jiang F, Kojima S, Zhao C and Feng C 2000 *J. Appl. Phys.* **88** 3608
[53] Bai Y, Xia Y, Li H, Han L, Wang Z, Wu X, Lv S, Liu X and Meng J 2012 *J. Phys. Chem. C* **116** 16841
[54] Deng Z, Kang C J, Croft M, Li W, Shen X, Zhao J, Yu R, Jin C, Kotliar G, Liu S, Tyson T A, Tappero R and Greenblatt M 2020 *Angew. Chem. Int. Ed.* **59** 8240
[55] Vasala S and Karppinen M 2015 *Prog. Solid State Chem.* **43** 1
[56] Zhang X W, Wang Q and Gu B L 1991 *J. Am. Ceram. Soc.* **74** 2846
[57] Setter N and Cross L E 1980 *J. Mater. Sci.* **15** 2478